ISSN 1063-7729, Astronomy Reports, 2011, Vol. 55, No. 12, pp. 1144–1154. © Pleiades Publishing, Ltd., 2011.
Original Russian Text © V.N. Obridko, A.A. Solov'ev, 2011, published in Astronomicheskii Zhurnal, 2011, Vol. 88, No. 12, pp. 1238–1248.

Magnetohydrostatic Model for a Coronal Hole

V. N. Obridko[1]* and A. A. Solov'ev[2]

[1] *N.V. Pushkov Institute of Terrestrial Magnetism, the Ionosphere, and Radio-Wave Propagation, Russian Academy of Sciences, Troitsk, Moscow Region, Russia*

[2] *Central (Pulkovo) Astronomical Observatory, Russian Academy of Sciences, Pulkovo, St. Petersburg, Russia*

Received May 12, 2011; in final form, June 15, 2011

Abstract—A model treating a solar coronal hole as an axially symmetrical magnetic formation that is in equilibrium with the surrounding medium is proposed. The model is applicable in the lower corona (to heights of the order of several hundreds of Mm), where the influence of the solar-wind outflow on the state of the system can still be neglected. The magnetic field of the coronal hole is comprised of a relatively weak open flux that varies with height, which extends into interplanetary space, and a closed field, whose flux closes at the chromosphere near the coronal hole. Simple analytical formulas are obtained, which demonstrate for a given equilibrium configuration of the plasma and field the main effect of interest—the lowering of the temperature and density of the gas in the coronal hole compared to their values in the corona at the same geometric height. In particular, it is shown that, at heights of several tens of Mm, the temperature and density of the plasma in the coronal hole are roughly half the corresponding values at the same height in the corona, if the cross-sectional radius of the hole exceeds the scale height in the corona by roughly a factor of 1.5: $R_h \approx 1.5H(T_0)$. In the special case when $R_h \approx H(T_0)$, the plasma temperature in the hole is equal to the coronal temperature, and the darkening of the coronal hole is due only to an appreciable reduction of the plasma density in the hole, compared to the coronal density. An analogy of the properties of coronal holes and sunspots is discussed, based on the similarity of the magnetic structures of these formations. In spite of the fundamental difference in the mechanisms for energy transport in coronal holes and sunspots, the equilibrium distributions of the plasma parameters in these formations are determined only by the magnetic and gravitational forces, giving rise to a number of common properties, due to their similar magnetic structures.

DOI: 10.1134/S1063772911120092

1. INTRODUCTION

Systematic studies of coronal holes (CHs) began in 1973–1974, based on data obtained with the Skylab space mission [1]. CHs are usually taken to be objects having brightnesses in the soft X-ray ($\lambda = 3$–60 Å) that are a factor of two to three lower than the surrounding corona, and temperatures $<10^6$ K. Beginning in 1975, CHs were observed with ground-based telescopes in the HeI 10830 Å line, in which they are brighter than the surrounding corona [2]. This is an absorption line, which becomes weaker in CHs, so that the emission present in the line is higher than in neighboring regions of the corona. It seems surprising that a line of neutral helium reacts to variations in the very hot corona. The reason is the population of the atomic level that determines the radiation in this line depends strongly on ionization by ultraviolet radiation with wavelengths shorter than 504 Å. The corona above the chromosphere where the neutral helium is located emits strongly in this region. This radiation, which arrives from above, is weakened in a CH (due to the joint action of the lower temperature and lower density), so that the population of the upper level of this triplet is reduced, leading to a decrease in the absorption. This mechanism is worked out in detail in [2–6]. At the base of a CH, both the temperature and the density apparently differ little from their values in the surrounding photosphere and chromosphere. Higher, beginning from a height of several tens of thousands of kilometers above the photosphere, the plasma temperature in the CH becomes appreciably lower than in the surrounding corona (being about 1–1.5 million K). The density is probably also lower in CHs, but estimates are somewhat discrepant [7].

Soft X-ray images of the Sun with high resolution have been regularly obtained with the Yohkoh satellite since 1991, and with the SOHO satellite since 1996. These data are published in the bulletin

*E-mail: obridko@mail.ru

"Solar-Geophysical Data" and can be accessed via the internet. These observations have revealed a number of important phenomenological properties of CHs, although their nature remains incompletely understood. CHs usually arise in unipolar regions with predominantly open magnetic-field configurations. A discussion of the physical conditions in typical CHs is given in [7, 8].

The main characteristics of CHs are formulated in "Solar-Geophysical Data" No. 644-1 (p. 94), as a basis for defining the shapes of CHs. Observed spectroheliograms in the HeI 10830 Å line and magnetograms of the photospheric magnetic field are used for this. Coronal holes are taken to be regions that:

(1) are brighter than the surrounding corona in observations of the HeI 10830 Å line,

(2) display a reduced contrast of the chromospheric network,

(3) are predominantly unipolar,

(4) have sizes no smaller than two supergranule cells, or $>6 \times 10^8$ km^2.

It is clear that these conditions are excessively strict, since there exist many CHs that satisfy only some of them. The reason is that the main physical definition of CHs is based on the fact that CHs are regions of open magnetic field. However, this property is efficiently manifest in the solar atmosphere only beginning from a certain height. The effect of the open magnetic-field configuration can be strongly blurred at lower altitudes, in the photosphere and chromosphere. It was shown in [9] that some regions on the Sun display only one of the identifying characteristics of CHs presented above. There exist regions of reduced contrast of the chromospheric network whose brightness does not differ from that of the surrounding background, and regions brighter than the surrounding background with high chromospheric-network contrasts.

The violation of the third characteristic that the regions be unipolar is fundamental. Unfortunately, this undoubtedly correct condition is often interpreted as implying unipolar fields at all levels, including the heights of the photosphere and chromosphere. In general, this is not valid, since closed loop magnetic structures are almost always present in the chromosphere and photosphere in the regions onto which the CH is projected.

Recently, Obridko and Shel'ting [10] analyzed 338 CHs distributed over all phases of the 23rd solar cycle. They calculated for all the CHs values of the index of unipolarity IU, defined as the ratio of the magnitude of the mean radial magnetic field B_R and its mean magnitude:

$$IU = |\langle B_R \rangle| / \langle |B_R| \rangle.$$

It is obvious that $IU = 1.0$ for a strictly unipolar field, while this value will be approximately zero in a multi-polar region. At heights of $1.1R_\odot$ (where $R_\odot$ is the solar radius), 281 CHs (i.e., 83%) had IU values of 0.9–1.0. This is consistent with the earlier result that CHs become predominantly unipolar formations by heights of $1.05R_\odot$ [11]. The internal structures of 18 CHs, likewise distributed over all phases of the 23rd solar cycle, were also studied in the 28.4 nm band. This showed that CHs contain both darker and less dark regions. The darkest regions have brightnesses less than 25% of the mean brightness of the disk at the given epoch. This is surrounded by a less dark region where the brightness is below 50% of the yearly-mean brightness at this wavelength. The darkest part of a CH corresponds to the region of maximum magnetic field, with the magnetic-field lines forming a weakly diverging bunch with inclinations to the vertical of no more than 20°. Outside the darkest part of a CH, the field lines can deviate more substantially from the normal direction.

This scheme is overall analogous to the picture proposed in 1988 by Wang et al. [12] to explain radio observations of CHs, and was later supported in [8, 13]. In 1996, Wang et al. [14] identified CHs with regions of open magnetic field. Further, these terms were applied to two equally important concepts of CHs, observed in the UV and X-ray at the disk and limb.

A large-scale magnetic field, CH, and active region form a single complex with the following properties in the process of their evolution.

Regions within which the magnetic field in the chromosphere and lower corona deviates from the radial direction by less than 20° lead to the appearance of optical and X-ray CHs. In spite of the physical identification of these two regions, some lack of coincidence of their boundaries is possible, as well as a delay in the appearance of the CH relative to the appearance of the region of open magnetic field.

Two to three rotations after their appearance, the shapes and sizes of CHs begin to change under the action of active regions located between conjugate CHs. As a result, a saddle-type configuration arises in the transverse field at the photospheric level near the boundary of the CHs.

The lifetimes of CHs, which comprise from two to three rotations to 1.5 years, exceed the lifetimes of the active regions associated with them. During the weakening or disappearance of these active regions, the CH changes accordingly.

The relationship between CHs and solar active regions was established in the study of Levine [15] based on Skylab data. It was later established [16, 17] that changes in the boundaries and energy balance

in CHs are determined to an appreciable extent by sporadic flows of hot ($T \approx 10^6$ K) plasma and regular inflows of energy from adjacent active regions.

Pneuman [18] showed that the inflow of energy into CHs is not necessarily lower than it is in regions of closed magnetic fields. The reduced brightness of CHs can be explained if the solar wind carries away a large fraction of this energy into the interplanetary medium.

It has been established that the magnetic fields in CHs expand with height in a super-radial fashion [19–21]. This means that the field lines deviate from the radial direction characteristic of a magnetic monopole. These deviations are relatively modest in the darkest regions of CHs, and do not exceed 20° at heights of $1.1R_\odot$ [8, 10, 22]. The UV and X-ray radiation is strongly reduced in this region, while the radiation at meter and decameter wavelengths is enhanced [12]. The deviations from the radial direction increase near the periphery of the CH, reaching 50°–70° [10].

2. ANALOGOUS PROPERTIES OF CORONAL HOLES AND SUNSPOTS

The above concepts lay at the basis of the suggestion of a close analogy between sunspots (as they are observed at the photospheric level) and CHs [13, 22]. One problem with this is that sunspots are associated with local and CHs with global magnetic fields. The essence of the analogy is that both of these types of object represent equilibrium magnetohydrostatic (MHS) structures with similar magnetic-field geometries. The mechanisms for the transport of thermal energy in CHs and in sunspots are completely different, but, in both cases, the equilibrium parameter distributions are determined only by the magnetic forces, their spatial distribution, and the gravitational force: since their magnetic-field structures are similar, we obtain similar distributions of the temperature and density.

It is precisely the similarity in the magnetic-field structure that provides the basis for this analogy. However, we can also identify a whole series of other analogous and common properties that are characteristic for these active solar formations.

At first glance, it appears to be an important difference between CHs and sunspots that the magnetic fields in sunspots reach values of 2000–3000 G, while the mean photospheric magnetic fields beneath CHs are only a few Gauss. However, we must remember that CHs are elements of the global field. Therefore, the situation changes as soon as we rise above the photosphere. The contribution of local field lines decreases sharply with height, and the magnetic field is already dominated by the contribution of large-scale elements at heights of several tenths of a solar radius. As a result, CHs are located at the positions of hills in the global magnetic field [22, 23]. For example, in the decay phase of the 22nd solar cycle in 1982–1985, 85% of CHs were located entirely or partially at the positions of maxima in the coronal magnetic field during the given solar rotation. Like sunspots, CHs have fairly sharp outlines that are determined by the strength of the magnetic field. Whereas the magnetic fields at the boundaries of sunspots are several hundred Gauss, the corresponding fields outlining the boundaries of CHs are 2–5 G.

The close connection between CHs and quasi-stable, high-speed solar-wind outflows [24, 25] is a consequence of the fact that CHs represent bunches of open field lines that deviate more appreciably from the normal direction with distance from the central parts of the CH [26–30]. Thus, CHs are located in regions of diverging field lines.

Figure 1 shows a map of the solar magnetic field at a height of $1.1R_\odot$ as a typical example; the center of this image corresponds to April 30, 2007. We can see that equatorial CHs can be located in regions of converging or diverging field lines. The magnetic-field lines in sunspot penumbrae behave in just the same way. As in sunspots, the flow of matter into CHs is channeled along the diverging field lines. The flow of matter from sunspots in the photosphere (the Evershed effect) comprises an outflow of matter at the photospheric level and an inflow at the chromospheric level. In CHs, outflows of matter are realized in the form of high-speed flows.

Another similarity between CHs and sunspots is that both types of object tend to group. Sunspots are usually joined into bipolar groups. An analogous effect is manifest in the distribution of CHs on the solar disk. CHs shifted from each other by ∼180° in longitude are often observed, with the magnetic fields in these CHs having opposite signs. An example of this situation is shown in Fig. 1.

Like sunspots, CHs are darker and cooler than their surroundings. In sunspots, the reduction in radiation compared to the surrounding photosphere arises due to cooling of the local plasma, as a consequence of the fact that the vertical magnetic field reduces the efficiency of convective heat transport from below. A CH is a dark formation compared to the surrounding corona in the UV and X-ray, but is brighter than its surroundings in the neutral helium line noted above. The contrast of CHs is due primarily to their lower temperatures, and only secondarily to their reduced plasma densities. The density deficit of the gas in the observed layers of sunspots leads to the formation of so-called Wilson depressions (the level of unit optical depth in the sunspot is located several hundred km below the photospheric level).

Fig. 1. Maps of the solar magnetic field at a height of $1.1R_\odot$ on April 30, 2007. In the map in the left panel, the arrows show the magnitude and direction of the transverse magnetic field and the circles show the bases of open field lines corresponding to the position of a CH on this day. A map of the radial magnetic field is shown in the central panel. The right panel shows an image of the Sun at 19.5 nm obtained on the same day. CHs are delineated by additional contours.

In most theories based on reconnection on small scales (DC models), the strength and complexity of the magnetic field is the main factor determining the dominant heating mechanism. Accordingly, the reduced energy fluxes of small elements in CHs are considered to be due to the reduction of the temperature and density in the CHs [31]. Another type of cooling mechanism related to magnetic fields—wave, or AC models—leads to an enhanced flux of waves, an outflow of matter, and cooling of the emitting gas (see the detailed review of Ashwanden [32]). Badalyan and Obridko [33, 34] showed that both types of mechanisms oerate in CHs, but their relative roles change somewhat with latitude. Thus, in both sunspots and CHs, their dark appearance is associated with plasma cooling and a density deficit, and the equilibrium state of these long-lived magneto-plasma systems is brought about by the similar structures of their magnetic fields.

Like sunspots, CHs have a central region that is darkest, whose brightness is lower than the yearly-mean solar brightness by a factor of four to five (the "umbra" of the CH), and an outer part where the brightness is below the mean by a factor of two to three (the "pemumbra" of the CH) [8, 10, 12, 13]. As in the umbra of a sunspot, the field lines deviate from the vertical only weakly in the darkest part of a CH.

Another curious parallel between CHs and sunspots is that the elemental abundances in the lower parts of CHs (the chromosphere, transition region, and lower corona) is very close to those that are observed in the photosphere [35, 36]. This sharply distinguishes CHs from other regions on the Sun, which display an appreciable enhancement in the abundances of elements with low first-ionization potentials (the FIP effect). This difference is preserved in the heliosphere, where high-speed flows and their associated CHs are often identified based on the similarity of their abundances of elements with low ionization potentials [37, 38].

Oscillations with periods of 10–30 min associated with compressions due to MHD waves propagating along the open field lines have been detected in CHs [39–41]. These oscillations, and also long-period oscillations (with periods from 1 to 3–4 h or longer) have also been detected in sunspots, in both the optical and radio [42–44].

All the characteristics listed above leave no doubt that there are close similarities between many properties of sunspots and CHs. It stands to reason that there cannot be a full physical analogy between these formations. First, their typical sizes differ by a factor of 10–30. Second, they are located in different layers of the solar atmosphere with different dominant heating mechanisms. However, as was noted above, the similarities between these long-lived active solar formations are brought about by the similarity in the structures of the magnetic fields forming them, which also determine the values of many other equilibrium parameters.

We note separately here the question of hydrostatic equilibrium in these objects. Outflows of matter are observed in both sunspots and CHs, and it would not be surprising if the distributions of matter in these outflows were appreciably non-MHS. However, this does not occur in either sunspots or in CHs. Obridko [45] presents numerous facts testifying to the validity of hydrostatic models for sunspots. Detailed modeling of the structure of a sunspot based on MHS equations [46, 47] provides a good agreement with modern empirical sunspot models [48]. Moreover, theoretical estimates [49] show that hydrostatic distributions are realized even in the sunspot penumbra, in spite of the presence of observationally striking plasma flows. Empirical models for sunspot penumbrae lead to the same conclusion [50]. At the same time, Badalyan [51] has convincingly shown that hydrostatic models for the density distribution are in agreement with observations of the white corona right out to heights of 2.5 solar radii; i.e., the solar wind

at these heights does not yet make a substantial contribution to the spatial structure of the density and temperature distributions.

3. MODELING THE MAGNETIC FIELD OF A CORONAL HOLE

A CH is a long-lived and slowly evolving magnetic formation, with the characteristic time scales for parameter variations substantially exceeding the time scales for establishing stationary distributions of parameters in the system. Therefore, we can neglect the partial derivative of the velocity with respect to time in the equation of motion of the plasma in a CH:

$$\rho(\mathbf{V}\nabla)\mathbf{V} = -\nabla P + \frac{1}{4\pi}[\mathrm{curl}\mathbf{B}\times\mathbf{B}] + \rho\mathbf{g}. \quad (1)$$

Moreover, if we limit our consideration to heights above the photosphere not exceeding $1-1.5R_\odot$, we can use an MHS approximation; i.e., we can completely neglect the inertial term in the left-hand side of (1). This approximation will obviously be valid if the square of the outflow velocity for the matter in the CH is appreciably smaller than the squares of the Alfvén velocity and of the sound speed:

$$V^2 \ll V_A^2 = \frac{B^2}{4\pi\rho}, \quad V^2 \ll c_s^2 = \frac{\gamma\Re T}{\mu}.$$

With a magnetic-field strength of several Gauss and a plasma density of 10^8-10^9 particles/cm^3, the Alfvén velocity in the corona is approximately 1000 km/s, and the sound speed for a temperature of about 1 MK is several hundred km/s. The velocity of the solar wind at the indicated heights is essentially undetectable, and is unlikely to exceed even 10 km/s. Thus, the inequality above is satisfied with a large margin, and the use of an MHS approximation to describe the structure of an equilibrium CH is fully justified.

The initial system of MHS equations takes the form

$$\frac{1}{4\pi}[\mathrm{rot}\,\mathbf{B}\times\mathbf{B}] - \nabla P + \rho\mathbf{g} = 0, \quad (2)$$

$$\mathrm{div}\mathbf{B} = 0, \quad (3)$$

$$P = \rho\frac{\Re T}{\mu}. \quad (4)$$

The first of these is the equilibrium equation for the system, the second the condition for the magnetic field to be solenoidal, and the third the equation of state of an ideal gas.

The magnetic field of an equilibrium CH can conveniently be represented as the sum of two static fields: $\mathbf{B}(r,z) = \mathbf{B}_1(r,z) + \mathbf{B}_2(r,z)$. The first of these, $\mathbf{B}_1$, is the field extending into interplanetary space in the form of a bunch of field lines with a fairly sharply bounded cross section, which varies with height relatively slowly, approximately according to an inverse-square law:

$$\mathbf{B}_1(r,z) = \frac{B_{0,1}}{1+(kr)^n}\frac{\mathbf{e}_z}{(1+z/R_\odot)^{2\varepsilon}} + B_{r,1}\mathbf{e}_r, \quad (5)$$

where $B_{0,1}$ is the strength of this field at the base of the CH at the point $r = 0$, $z = 0$ (we use here a cylindrical coordinate system r, φ, z (Fig. 2) related to the assumed symmetry axis of the CH); $B_{r,1}$ is the radial component of this field; n is a positive numerical index that must be chosen to be large enough to ensure a sharp spatial boundary and uniformity of the density and temperature distributions across the CH cross section (we adopted $n = 20$ for our numerical calculations); and ε is a positive coefficient that is close to unity ($\varepsilon \geq 1$), which can be used to take into account the modest deviation of the variation of the field with height from an inverse-square law. Finally, the parameter k is the inverse transverse scale for the field $\mathbf{B}_1$. It is obvious that $kR_\odot \gg 1$ (it is approximately 10–20), so that, we can show using the condition $\mathrm{div}\mathbf{B} = 0$ that $B_{r,1} \ll B_{z,1}$; consequently, the influence of the radial component of the field $B_{r,1}$ on the force balance in the system can be neglected.

The second field $\mathbf{B}_2(r,z)$ has a potential distribution that falls off exponentially with height, of the form

$$\mathbf{B}_2(r,z) = B_{0,2}J_0(\alpha r)\exp(-\alpha z)\mathbf{e}_z + B_{0,2}J_1(\alpha r)\exp(-\alpha z)\mathbf{e}_r. \quad (6)$$

Here, $B_{0,2}$ is the strength of this magnetic field at the coordinate origin, $J_0(\alpha r)$ and $J_1(\alpha r)$ are zeroth- and first-order Bessel functions of the first kind, and $\alpha = \mathrm{const}$ is the inverse scale length for the field $\mathbf{B}_2$.

It can easily be shown via a direct substitution that the magnetic field (6) satisifies both the solenoidal condition $\mathrm{div}\mathbf{B} = 0$ and the potential condition $\mathrm{curl}\mathbf{B} = 0$. We suggest that this distribution, with its oscillating "tails" that slowly fall off with radius, successfully imitates not only the magnetic field inside a CH, but also the "magnetic carpet" in the vicinity of the CH.

The sum of the two fields, $\mathbf{B}_1 + \mathbf{B}_2$, yields a magnetic-rosette-type coronal magnetic configuration, in which the main magnetic flux returns to the chromosphere and a relatively weak, weakly diverging central bunch of field lines emerges outward vertically upward into the corona. Qualitatively, this represents the magnetic structure of a CH, whose general form resembles that of a sunspot, as is depicted in Fig. 2.

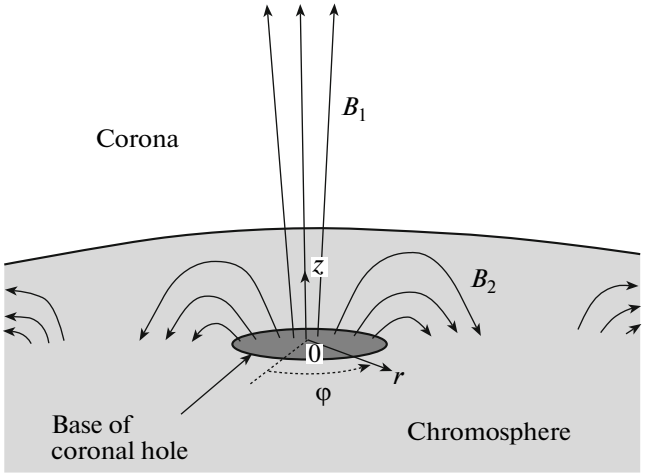

Fig. 2. Qualitative appearance of a magnetic configuration described by the fields $\mathbf{B}_1 + \mathbf{B}_2$. A cylindrical coordinate system r, φ, z is shown.

The magnetic force due to the resulting field $\mathbf{B}_1 + \mathbf{B}_2$ will have two components:

$$\mathbf{F}_m = \frac{1}{4\pi}\,[\mathrm{curl}\mathbf{B} \times \mathbf{B}] \tag{7}$$
$$= \frac{1}{4\pi}\,[\mathrm{curl}\mathbf{B}_1 \times (\mathbf{B}_1 + \mathbf{B}_2)]$$
$$= \frac{\mathbf{e}_r}{4\pi}\left(-B_{z,1}\frac{\partial B_{z,1}}{\partial r} - B_{z,2}\frac{\partial B_{z,1}}{\partial r}\right) + \frac{\mathbf{e}_z}{4\pi}\left(B_{r,2}\frac{\partial B_{z,1}}{\partial r}\right).$$

4. MAGNETOHYDROSTATIC SOLUTIONS FOR A CORONAL HOLE

MHS problems are usually formulated in terms of the magnetic flux of the vertical field $\Psi(r, z)$. The Grad–Shafranov equation [52] is derived from the equilibrium condition, a specific dependence of the gas pressure on the flux $\Psi(r, z)$ is specified based on some additional considerations (usually of a purely mathematical nature), and the resulting differential equation in the function $\Psi(r, z)$ is solved; i.e., a solution for the magnetic structure of the equilibrium configuration is found. This is the so-called direct problem. Of no less interest is the corresponding inverse problem [53, 54], when a specified magnetic-field structure is used to determine the distributions of the pressure, density, and temperature corresponding to the equilibrium conditions for the specified magnetic field. These are in fact the parameters that can be derived from coronal measurements, whereas it is not possible to directly measure magnetic fields in the solar corona. For this reason, it is this inverse MHS problem that we consider in describing a long-lived equilibrium CH.

As was noted above, we limit our consideration to relatively low heights ($z < R_\odot$), where the outflow of plasma from the region of the CH (the solar wind) is modest, and its influence on the main parameters of the CH can be neglected.

We write the equilibrium condition of the plasma (2) in terms of components:

$$-\frac{\partial P}{\partial z} + \frac{B_{0,2}}{4\pi}J_1(kr)\exp(-kr)\frac{\partial B_{z,1}}{\partial r} - \rho g = 0, \tag{8}$$

$$-\frac{\partial P}{\partial r} - \frac{1}{4\pi}\left[\frac{1}{2}\frac{\partial B_{z,1}^2}{\partial r} + B_{0,2}J_0(kr) \times \exp(-kr)\frac{\partial B_{z,1}}{\partial r}\right] = 0. \tag{9}$$

The first of these equations serves to determine the plasma density $\rho(r, z)$ at the point of the magnetic configuration of interest to us, and the second to calculate the pressure $P(r, z)$ for a specified magnetic structure. To find the pressure $P(r, z)$, we integrate (9) over the radius from ∞ to r; i.e., beginning from a very distant point where the influence of the CH magnetic field on the state of the plasma can be neglected to some point located a distance r from the axis of symmetry of the system. We obtain:

$$-P(r, z) + P_0(z) - \frac{B_{z,1}^2(r, z)}{8\pi} - \frac{B_{0,2}}{4\pi}\exp(-kz)\int_\infty^r J_0(kr)\frac{\partial B_{z,1}}{\partial r}dr = 0,$$

where $P_0(z)$ is the unperturbed hydrostatic pressure far from the CH. Further, using the obvious relation

$\int_\infty^r f dr = -\int_r^\infty f dr = -\int_0^\infty f dr + \int_0^r f dr$, we find

$$P(r,z) = P_0(z) - \frac{B_{0,1}^2}{8\pi}\frac{1}{(1+(kr)^n)^2} \times \frac{1}{(1+z/R_\odot)^{4\varepsilon}} + \frac{B_{0,2}}{4\pi}\exp(-\alpha z) \times \left(\int_0^\infty J_0(\alpha r)\frac{\partial B_{z,1}}{\partial r}dr - \int_0^r J_0(\alpha r)\frac{\partial B_{z,1}}{\partial r}dr\right).$$

We calculate the integrals in parantheses by parts, taking into account the fact that $J_0' = -J_1$. We then obtain

$$P(r,z) = P_0(z) - \frac{B_{0,1}^2}{8\pi}\frac{1}{[1+(kr)^n]^2} \times \frac{1}{(1+z/R_\odot)^{4\varepsilon}} + \frac{B_{0,1}B_{0,2}}{4\pi}\frac{\exp(-\alpha z)}{(1+z/R_\odot)^{2\varepsilon}}F(r), \quad (10)$$

where $F(r) = -\frac{J_0(\alpha r)}{1+(kr)^n} + \int_0^\infty \frac{J_1(\alpha r)}{1+(kr)^n}d(\alpha r) - \int_0^{\alpha r}\frac{J_1(\alpha r)}{1+(kr)^n}d(\alpha r)$.

Substituting (10) into (8), we obtain an expression for the gas density in the CH, and then find the gas temperature in the CH from the ideal-gas equation of state (4) and the already known pressure and density. Thus, the problem of determining the pressure, density, and temperature of the plasma at any point of the equilibrium magneto-plasma system considered here based on a specified structure for its magnetic field is solved.

5. QUANTITATIVE ANALYSIS AND DISCUSSION

We will now present numerical calculations for various relationships between the geometrical dimensions α and k, all with $n = 20$: $\alpha_1 = 0.75k$, $\alpha_2 = k$, and $\alpha_3 = 1.25k$. As was noted above, the higher the index n, the sharper the boundary of the CH. The degree of uniformity of the cross-sectional distributions of the temperature and density in the CH are determined by the ratio α/k: the closer this ratio is to unity, the more uniform these distributions will be. Figure 3 presents $F(r)$, which has the form of a nearly rectangular step function when $\alpha = k$: near the axis of the CH, when $x \equiv kr < 1$, this function is equal to -0.762, and it increases in a nearly jump-like fashion to zero when $x \equiv kr > 1$, retaining this value upon further increase in the distance from the axis. When $\alpha \neq k$, the profile of the base of the CH becomes uneven, rising toward the center for $\alpha < k$ and decreasing toward the center for $\alpha > k$. Figure 3 also shows the Bessel functions $J_0(x)$ and $J_1(x)$.

Further, we will assume that $\alpha \equiv k$, i.e., that the vertical and horizontal scales of our magnetic structure coincide; this is precisely the condition for the base of the CH to be flattest. Taking into account the characteristic form of the function $F(r)$, we can write for the region internal to the CH (i.e., for $kr < 1$):

$$P(r,z) = P_0(z) - \frac{B_{0,1}^2}{8\pi}\frac{1}{[1+(kr)^n]^2} \times \frac{1}{(1+z/R_\odot)^{4\varepsilon}} - 1.524\frac{B_{0,1}B_{0,2}}{8\pi}\frac{\exp(-kz)}{(1+z/R_\odot)^{2\varepsilon}}. \quad (11)$$

Substituting this expression into (8) yields the spatial distribution fo the plasma density in the CH:

$$\rho(r,z) = \rho_0(z) - \frac{B_{0,1}^2}{8\pi g R_\odot}\frac{1}{[1+(kr)^n]^2} \times \frac{4\varepsilon}{(1+z/R_\odot)^{4\varepsilon+1}} - \frac{1.524B_{0,1}B_{0,2}}{8\pi g} \times \frac{\exp(-kz)}{(1+z/R_\odot)^{2\varepsilon}}\left[k + \frac{1}{(1+z/R_\odot)R_\odot}\right] - \frac{B_{0,1}B_{0,2}}{4\pi g}\frac{J_1(kr)20k(kr)^{19}\exp(-kz)}{[1+(kr)^{20}]^3(1+z/R_\odot)^{2\varepsilon}}. \quad (12)$$

The strength of the open field $\mathbf{B}_1$ should be appreciably lower than that of the lower-lying field $\mathbf{B}_2$, since, at sufficient heights, the transverse pressure of the open field $\mathbf{B}_1$ must be balanced by the very weak pressure of the coronal plasma. This suggests that $B_{0,1}$ should not exceed fractions of a Gauss, whie the closed field $B_{0,2}$ is several Gauss. Based on this reasoning and the fact that $kR_\odot \gg 1$, and that $(kr)^{19} \ll 1$ everywhere inside the CH, we can with good accuracy distinguish two main terms in (11) and (12):

$$P(r,z) \cong P_0(z) - \frac{B_{0,1}B_{0,2}}{8\pi}Y(z), \quad (13)$$

$$\rho(r,z) \cong \rho_0(z) - \frac{B_{0,1}B_{0,2}}{8\pi g}kY(z). \quad (14)$$

where $Y(z) = 1.524\exp(-kz)(1+z/R_\odot)^{-2\varepsilon}$. We can write using the ideal-gas equation of state (4):

$$\frac{P}{\rho g} = \frac{\Re T}{\mu g} \equiv H(T), \quad (15)$$

where $H(T)$ is the scale height for a uniform atmosphere. It follows from (13)–(15) that

$$H(T_0)\frac{T(z)}{T_0(z)} = \frac{P_0(z) - \frac{B_{0,1}B_{0,2}}{8\pi}Y(z)}{\rho_0(z)g - k\frac{B_{0,1}B_{0,2}}{8\pi}Y(z)}. \quad (16)$$

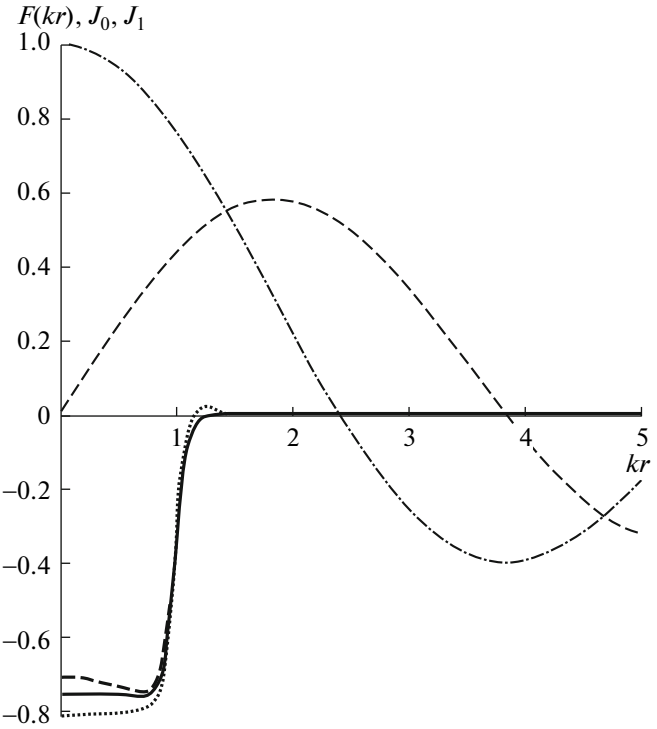

Fig. 3. Appearance of the function $F(kr)$ for three different cases, shown by the three nearly merging curves: $\alpha_1 = 0.75k$ (top curve), $\alpha_2 = k$ (middle curve), and $\alpha_3 = 1.25k$ (bottom curve). The thin dash–dotted and dashed curves shown the functions $J_0(x)$ and $J_1(x)$, respectively.

Here, $T_0(z)$ is the temperature in the solar corona that is free of the CH magnetic field at a specified geometric height and $H(T_0)$ is the scale height for a uniform atmosphere corresponding to the temperature T_0. Further, we introduce the notation for the plasma parameter (which is a function of height in this case)

$$\beta_0(z) = \frac{P_0(z)8\pi}{B_{0,1}B_{0,2}Y(z)}. \qquad (17)$$

Note that $\beta_0(z) > 1$ in this model. Otherwise, according to (13) and (16), the plasma pressure and temperature turn out to be negative. Using the relation $\rho_0(z)gH(T_0) = P_0(z)$ and relations (14) and (16), we obtain for the temperature and density inside the CH in units of the temperature and density of the surrounding medium at the same geometric height the simple expressions

$$\frac{T(z)}{T_0(z)} = \frac{\beta_0(z) - 1}{\beta_0(z) - kH(T_0)}, \qquad (18)$$

$$\frac{\rho(z)}{\rho_0(z)} = 1 - \frac{kH(T_0)}{\beta_0(z)}. \qquad (19)$$

As we can see, the dominant role in determining the distributions of the temperature and gas density in an equilibrium CH is played by the quantity $kH(T_0)$, which is the ratio of the scale height in the corona to the radius of the CH ($k = R_h^{-1}$): $kH_0(T) = R_h^{-1}H_0(T)$. Since $\beta_0(z) > 1$, the satisfaction of only one purely geometrical condition is sufficient to obtain the main effects manifest by the CH (a reduction of the temperature compared to the coronal temperature at the same geometric height):

$$kH(T_0) < 1$$

(or $H_0(T) < R_h$). We emphasize that the resulting effect is very general and stable in the sense that its sign does not depend on any quantitative estimates and the physical parameters of the coronal plasma, apart from the temperature. If $kH(T_0) = 1$, the plasma temperatures in the CH and in the corona are equal; when $\beta_0 > kH(T_0) > 1$, the gas temperature in the CH is even somewhat higher than the coronal temperature. (As we can see from (18), if $kH(T_0) = \beta_0$, the temperature of the CH becomes infinitely high and an equilibrium state is not possible in the system. Equilibrium is likewise impossible when $kH(T_0) > \beta_0$, since this leads to negative temperatures.)

For very large CHs, when $kH(T_0) \ll \beta_0$, the associated maximally reduced plasma temperature in the

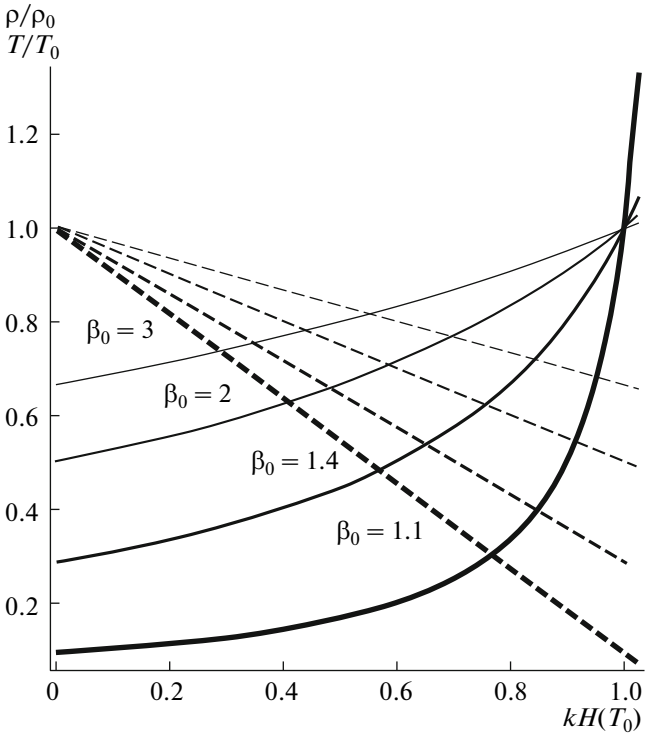

Fig. 4. Dependence of the relative temperature $T(z)/T_0(z)$ (solid curves) and density $\rho(z)/\rho_0(z)$ (dashed curves) of the gas in a CH on $kH(T_0)$ for various values of the plasma parameter β_0. The thickness of the curve increases with decreasing β: the thickest curves correspond to $\beta_0(z) = 1.1$ and the thinnest ones correspond to $\beta_0(z) = 3$.

CH is

$$\frac{T(z)}{T_0(z)} = 1 - \frac{1}{\beta_0(z)}. \qquad (20)$$

However, according to (19), $\rho(z) = \rho_0(z)$, i.e., the CH will be due only to the difference in the temperatures of the CH and corona. For example, if we adopt $\beta_0(z) = 2$, then $T(z) = 0.5T_0(z)$. In another important special case, when $kH(T_0) = 1$, according to (18), the temperature difference between the CH and corona vanishes, but the density difference turns out to be appreciable:

$$\frac{\rho(z)}{\rho_0(z)} = 1 - \frac{1}{\beta_0(z)}, \qquad (21)$$

so that, in this case, the darkening of the CH in the UV and X-ray is due exclusively to the reduction of the plasma density in the CH. It was found in [55] based on Yohkoh X-ray data that the gas temperature in a CH, 1.8–2.4 MK, was not significantly lower than the coronal temperature, while the emission in the CH was lower by an order of magnitude—obviously due to the fact that the plasma density in the CH was lower by about a factor of three compared to the coronal density. If we assume for the CH studied in [55] that $kH(T_0) = 1$, then, according to (21), we find that the corresponding plasma parameter is $\beta_0(z) = 1.5$, which seems an entirely reasonable estimate. (It is interesting that the relative temperatures and densities in CHs given by (20) and (21) quantitatively coincide.) Figure 4 shows the dependences (18) and (19) for various values of the plasma parameter.

The scale height for a uniform atmosphere in the chromosphere does not exceed several thousand km, so that the condition $H(T_0) < R_h$ is easily satisfied. Due to the sharp increase in the temperature with height to approximately 1–1.5 MK, the scale height in the corona $H(T_0)$ likewise grows to 50–75 Mm. Therefore, CHs at coronal heights with such temperatures cannot have sizes smaller than the indicated value.

Let us consider another quantitative estimate. At a height of 40–50 Mm, $P_0(z) \approx 0.1$ dyne/cm^2, $T_0(z) \approx 10^6$ K, and $Y(z) \approx 0.7$. If we adopt $B_{0,1} \approx 0.5$ G and $B_{0,2} \approx 5$ G, we obtain $\beta_0(z) \approx 1.4$. The scale height in the corona at this level is about 50 Mm, and we estimate for the radius of a typical large-scale CH $R_h \approx 75$ Mm. In this case, $kH(T_0) = 0.667$, and, according to (18) and (19), $\frac{T(z)}{T_0(z)} \approx 0.545$, $\frac{\rho(z)}{\rho_0(z)} \approx 0.524$; i.e., both the temperature and the density of the plasma in the CH are a factor of two lower than their coronal values at the same geometric height.

In absolute units, the temperature is approximately 0.5 MK and the plasma number density in the CH is a few times 10^8 particles/cm^3.

Note that the analogy with sunspots described above can be traced in the temperature distribution in the CH given by (18). The scale height is small in a sunspot at the photospheric level (only about 130 km), so that $kH(T_0) \ll 1$, and the equilibrium sunspot is appreciably cooler than the photosphere. However, $H(T_0)$ grows rapidly when higher layers are reached, and becomes comparable to and then greater than the magnetic scale height, so that $kH(T_0) > 1$ at heights of several thousand km in the upper chromosphere and lower corona, where the plasma above the sunspot is now hotter than the surrounding medium (it is sometimes said in this regard that "the corona begins earlier above a sunspot", i.e., the lower boundary of the corona is lower than in the unperturbed state outside the sunspot).

6. CONCLUSION

We have described a number of common properties inherent to CHs and sunspots. This analogy can be explained by the similarity of the magnetic structures of these objects. In the equilibrium state, the spatial distributions of the temperature and density depend only on the magnetic and gravitational forces. When the magnetic structures of two formations are similar, the temperature and density characteristics of the two equilibrium magneto-plasma systems are also similar, in spite of the substantial difference in their heat-transport mechanisms.

The magnetic field in the proposed model for a CH is similar to the field of a sunspot, in the form of a "rosette" whose main magnetic flux returns to the chromosphere in the immediate vicinity of the CH, but with a relatively small fraction of the magnetic flux from the central part of the CH emerging from the corona into interplanetary space, thus serving as a channel along which the high-speed solar-wind flow forms at sufficiently large heights.

We have calculated the parameters of a CH in a magnetohydrostatic approximation (taking into account the gravitational force). The influence of plasma flows on the structure of the CH was not included. This approximation is fully justified, at least to heights of the order of the solar radius above the level of the photosphere.

The main effect distinguishing CHs—a reduced temperature compared to the coronal value—can be explained purely by a geometrical condition: the cross-sectional radius of the CH must exceed the scale height in the corona at the corresponding level ($R_h > H(T_0)$). The sign of this effect does not depend on any quantitative estimates, apart from the temperature of the surrounding corona and the parameters of the CH and coronal plasma. The typical density and temperature distributions of CHs agree well with observations: the temperature and density of the gas in CHs at heights of several tens of Mm are roughly half their coronal values.

According to our proposed model, when the cross-sectional radius of a CH is close to the scale height in the corona ($R_h = H(T_0)$), the gas temperature in the CH is comparable to the coronal temperature, and the darkening of the CH is due purely to an appreciable reduction of the plasma density in the CH compared to the coronal density.

ACKNOWLEDGMENTS

This work was supported by the Basic Research Program of the Division of Physical Sciences of the Russian Academy of Sciences OFN-15, the Basic Research Program of the Presidium of the Russian Academy of Sciences P-19, and the Russian Foundation for Basic Research (project 11-02-00259).

REFERENCES

1. *Coronal Holes and Highspeed Wind Streams*, Ed. by J. B. Zirker (Colorado Assoc. Univ. Press, Boulder, USA, 1977).
2. J. Harvey, A. S. Krieger, A. F. Timothy, and G. S. Vaiana, Mem. Osserv. Astrofis. Arcetri **104**, 50 (1975).
3. K. L. Harvey and F. Recely, Solar Phys. **211**, 31 (2002).
4. H. Zirin, Astrophys. J. **199**, L63 (1975).
5. V. Andretta and H. P. Jones, Astrophys. J. **489**, 375 (1997).
6. R. Centeno, J. Trujillo Bueno, H. Uitenbroek, and M. Collados, Astrophys. J. **677**, 742 (2008).
7. S. R. S. Cranmer, Living Rev. Solar Phys. **6**, No. 3 (2009).
8. E. I. Mogilevsky, V. N. Obridko, and N. S. Shilova, Solar Phys. **28**, 247 (1997).
9. E. V. Malanushenko, V. P. Malanushenko, and N. N. Stepanyan, Izv. RAN, Ser. Fiz. **59**, 38 (1995).
10. V. N. Obridko and B. D. Shelting, Solar Phys. **270**, 297 (2011).
11. O. I. Bugaenko, I. A. Zhitnik, A. P. Ignat'ev, et al., Izv. Krymsk. Astorofiz. Observ. **100**, 123 (2004).
12. Z. Wang, M. R. Kundu, and H. Yoshimura, in *Solar and Stellar Coronal Structure and Dynamics,* A89-20526 06-92 (Nat. Solar Observ., Sunspot, NM, USA:, 1988), p. 458.
13. V. N. Obridko, in *Advances in Solar Connection with Transient Interplanetary Phenomena*, Ed. by X. H. Feng, F. S. We, and M. Dryer (Internat. Acad. Publs., Beijing, 1998), p. 41.
14. Y.-M. Wang, S. H. Hawley, and N. R. Sheeley, Jr., Science **271**, 464 (1996).
15. R. H. Levine, Astrophys. J. **218**, 291 (1977).

16. K. Shibata, T. Jokoyamaand, and M. Shimojo, in *New Look at the Sun with Emphasis on Advanced Observations of Coronal Dynamics and Flares,* Ed. by S. Enome and T. Hirayama, NRO Rep. No. 360 (Nobeyama Radio Observatory, Nagano, Japan, 1994), p. 75.
17. E. I. Mogilevsky, Geomagn. Aeron. **35**, 11 (1995).
18. G. W. Pneuman, Solar Phys. **28**, 247 (1973).
19. V. A. Kovalenko, *Solar Wind* (Nauka, Moscow, 1983) [in Russian].
20. Y.-M. Wang and N. R. Sheeley, Jr., Astrophys. J. **355**, 726 (1990).
21. Y.-M. Wang, N. R. Sheeley, Jr., and A. G. Nash, Nature **347**, 439 (1990).
22. V. N. Obridko and B. D. Shelting, Solar Phys. **124**, 73 (1989).
23. V. N. Obridko and B. D. Shel'ting, Sov. Astron. **34**, 449 (1990).
24. J. M. Wilcox, Space Sci. Rev. **8**, 258 (1968).
25. A. S. Krieger, A. F. Timothy, and E. C. Roelof, Solar Phys. **29**, 505 (1973).
26. M. Guhathakurta, E. Sittler, R. Fisher, et al., Geophys. Res. Lett. **26**, 2901 (1999).
27. S. R. Cranmer, J. L. Kohl, G. Noci, et al., Astrophys. J. **511**, 481 (1999).
28. H. P. Jones, in *Large-scale Structures and Their Role in Solar Activity,* Ed. by K. Sankarasubramanian, M. Penn, and A. Pevtsov, ASP Conf. Proc. **346**, 229 (2005).
29. Y.-M. Wang and N. R. Sheeley, Jr., Astrophys. J. **653**, 708 (2006).
30. Y.-M. Wang, J. B. Biersteker, N. R. Sheeley, et al., Astrophys. J. **660**, 882 (2007).
31. R. Rosner, W. H. Tucker, and G. S. Vaiana, Astrophys. J. **220**, 643 (1978).
32. M. J. Aschwanden, *Physics of the Solar Corona: An Introduction* (Springer, Praxis Publ., Berlin, Chichester, 2004).
33. O. G. Badalyan and V. N. Obridko, Solar Phys. **238**, 271 (2007).
34. O. G. Badalyan and V. N. Obridko, Astron. Lett. **33**, 182 (2007).
35. U. Feldman, Space Sci. Rev. **85**, 227 (1998).
36. U. Feldman and K. G. Widing, Space Sci. Rev. **107**, 665 (2003).
37. R. von Steiger, R. F. Wimmer-Schweingruber, J. Geiss, and G. Gloeckler, Adv. Space Res. **15**, 3 (1995).
38. T. H. Zurbuchen, L. A. Fisk, G. Gloeckler, and R. von Steiger, Geophys. Res. Lett. **29**, 1352 (2002).
39. C. E. De Forest and J. B. Gurman, Astrophys. J. **501**, L217 (1998).
40. L. Ofman, V. M. Nakariakov, and C. E. De Forest, Astrophys. J. **514**, 441 (1999).
41. L. Ofman, M. Romoli, G. Poletto, et al., Astrophys. J. **529**, 592 (2000).
42. V. I. Efremov, L. D. Parfinenko, and A. A. Solov'ev, Astron. Rep. **84**, 401 (2007).
43. V. I. Efremov, L. D. Parfinenko, and A. A. Solov'ev, Solar Phys. **267**, 279 (2010).
44. O. G. Badalyan, V. N. Obridko, Ya. Rybak, and Yu. Sykora, Astron. Rep. **51**, 659 (2005b)].
45. V. N. Obridko, *Sunspots and Activity Complexes* (Nauka, Moscow, 1985) [in Russian].
46. A. A. Solov'ev, Astron. Rep. **41**, 131 (1997).
47. A. A. Solov'ev, Astron. Rep. **42**, 110 (1998).
48. M. Collados, V. M. Pullet, B. R. Cabo, et al., Astron. Astrophys. **291**, 622 (1994).
49. A. A. Solov'ev and E. A. Solov'eva, Astron. Lett. **23**, 277 (1997).
50. O. K, Moe and P. Maltby, Solar Phys. **8**, 275 (1969).
51. O. G. Badalyan, Astron. Astrophys. Trans. **9**, 205 (1996).
52. L. D. Landau and E. M. Lifshitz, *Course of Theoretical Physics,* Vol. 8: *Electrodynamics of Continuous Media* (Nauka, Moscow, 1982; Pergamon, New York, 1984).
53. B. C. Low, Solar Phys. **65**, 147 (1980).
54. A. A. Solov'ev, Astron. Rep. **54**, 86 (2010).
55. H. Hara, S. Tsuneta, L. W. Acton, et al., Adv. Space Res. **17**, 231 (1996).

Translated by D. Gabuzda